Anatomy of three-body decay II. Decay mechanism and resonance structure

E. Garrido

Instituto de Estructura de la Materia, CSIC, Serrano 123, E-28006 Madrid, Spain

D.V. Fedorov, A.S. Jensen and H.O.U. Fynbo

Department of Physics and Astronomy, University of Aarhus, DK-8000 Aarhus C, Denmark

Abstract

We use the hyperspherical adiabatic expansion method to discuss the the two mechanisms of sequential and direct three-body decay. Both short-range and Coulomb interactions are included. Resonances are assumed initially populated by a process independent of the subsequent decay. The lowest adiabatic potentials describe the resonances rather accurately at distances smaller than the outer turning point of the confining barrier. We illustrate with realistic examples of nuclei from neutron (^{6}He) and proton (^{17}Ne) driplines as well as excited states of beta-stable nuclei (^{12}C).

PACS: 21.45.+v, 31.15.Ja, 25.70.Ef

1 Introduction.

Resonance states consisting of a number of particles may decay into final states of many fragments. Prominent examples are α-decay, nucleon emission and binary fission, where only two clusters are present after the decay. The next step is three particles in the final state which has been studied in various connections for many years, see e.g. [1]. The recent years has witnessed enormous progress in the treatment of the many possible three-body structures [2]. As usual the continuum problem has turned out to be more difficult, e.g. the first computation with the correct boundary condition for decay into three charged particles is less than 10 years old [3].

The experimental techniques have developed tremendously the later years and more details, accuracy and systematics are available for different decays. In particular the complicated structures, where both Coulomb and short-range interactions are crucial, now begin to attract increasing attention especially in the discussion of two-proton radioactivity. Experimental information accumulates both for ground state two-proton decay of unstable systems along the proton dripline [4–6] and for excited states of more stable nuclei [7–10]. The analyses and interpretations of the three-body decay experiments are essentially all consistent with sequential decay [7–10]. Direct decay into three-body continuum states is in principle always possible and perhaps preferred, for example for short-lived intermediate resonances or when sequential decay is forbidden by energy conservation.

Different types of calculations with the focus on three-body decay widths are now available, e.g. using R-matrix theory where only two sequential two-body emissions is included [11], R-matrix theory combined with microscopic shell model computations with the inherent model restrictions [12], three-body models with outgoing flux where essentially only direct decay to the continuum is included [13], three-body models with Faddeev type of components combined with complex coordinate scaling [14], or from the Faddeev equations combined with either outgoing flux or complex scaling [15]. The three-body models have very restricted model spaces but are precisely tuned to describe three-body structures.

Let us now consider a decaying resonance with complex energy where the real and imaginary parts define the position and the partial three-body decay width, respectively. We assume that the decay is independent of the formation as for lifetimes long compared to the population process. If the initial state is a many-body resonance the three fragments in the final state must be created as part of the decay process. Using three-body models this opens for a definition of three-body spectroscopic factors in analogy to the preformation factors used for α-decay [16]. This tacitly assumes, as for α-decay, that the small distance many-body dynamics is unimportant for the process. Similarly defined spectroscopic factors can be computed with the shell-model [11], where a non-stationary final state seems to be present after the decay..

The decay process leads from an initial to a final state of separated particles. Outside the range of the strong interaction only the Coulomb and centrifugal barriers remain. However, different paths to the final-state of three free particles are still possible, e.g. sequential decay or direct decay into the three-particle continuum. In the preceding companion paper we discussed the relative importance of these decay mechanisms in a schematic model where the short-range interaction only is used to provide the correct resonance energy [17].

The most advanced three-body models include both aspects in resonance computations, where the correct asymptotic large distance boundary conditions are properly accounted for by a complex energy or by complex rotation [3,18–20]. The intermediate configurations attempting to describe the process are non-observables. Virtual population of such states can only be indicated through a model interpretation. A distinction of decay mechanism could then be rather uninteresting and perhaps even impossible. However, characterization of the reaction mechanism is essential to understand a given process and indispensable for generalizations to other processes, systems and observables. In any case a rigorous distinction between sequential and direct decays is not meaningful without clear definitions.

The purpose of the present paper is to investigate the mechanism for three-body decay from (possibly) many-body resonances. We shall focus on how the resonance wave functions are related to the decay mechanisms which in turn produce for example the observable energy spectra. We shall report on elaborate computations for realistic nuclear systems with both short and long-range interactions. We intent to bridge the gap between theory and the dominating experimental analysis in terms of sequential decay.

2 Resonances and the decay mechanisms

Characteristic properties of a given system are revealed by the complex poles of its S-matrix. Poles of purely real, negative energy on the physical and unphysical Riemann sheet correspond to bound states and virtual states, respectively. Poles with complex energies, $E = E_r - i\Gamma/2$, correspond to resonances of energy E_r and width Γ. A peak structure of given position and width for a specific observable can then be related to E_r and Γ. We shall first compute energies for the poles of the resonances. The decay widths Γ are then available and the corresponding wave functions carry information about the decay mechanism.

2.1 General method

We use the hyperspherical adiabatic expansion of the Faddeev equations [21] for the three particles appearing in the final state after the decay. This means that we first must determine the interactions V_{ij} reproducing the low-energy two-body scattering properties. Here the two-body bound and virtual states and the resonances are possible fixpoints if the phase shifts are unavailable in the desired region of energies.

A three-body short-range interaction depending on the coordinates of all three particles may in addition be needed for example when the precise resonance energy is required. This interaction may be very small and amount to fine-tuning of the energy, but it could also be substantial if the resonance at small distances is far from the three-body structure appearing after the decay. A relatively large three-body interaction is usually needed when a many-body resonance decays into three fragments.

The effects of the three-body potential are changes of the (i) real part of the energy to the desired value, which most effectively is achieved with the strength, (ii) imaginary part of the resonance energy achieved by reduction of the barrier, which is sensitive to the range of the interaction, (iii) expansion coefficients of the radial wave function on the adiabatic components, which only can be strongly modified by a dependence on the quantum numbers of each adiabatic wave function. With a three-body potential which only depends on the hyperradius, the short-range property then ensures that the decay mechanism remains almost independent of strength and range.

We use hyperspherical coordinates as for example defined in [17]. For fixed hyperradius, ρ, we then first solve the angular Faddeev equations to obtain the adiabatic potentials, see examples for the diagonal parts in Fig. 1. All these potentials diverge for small ρ due to the generalized centrifugal barrier and vanish for large ρ at least as ρ^{-3} for the short-range interaction of ^{6}He and as $1/\rho$ for the Coulomb potential for ^{12}C [21]. At relatively small distance the attraction leads to minima responsible for bound states and resonance structures.

The total wave function is expanded on the angular eigenfunctions where the ρ-dependent expansion coefficients are the hyperradial wave functions. They are obtained from the resulting set of coupled hyperradial equations solved with the boundary conditions appropriate for the problem under investigation. Virtual states and resonances can then in principle be found by the conditions of outgoing fluxes in all channels. This requires a complex energy which then is the resonance position and width. The precise computation with this complex energy method is in practice numerically delicate [22].

Another much more efficient method is to "rotate" all the coordinates by the same angle into complex values like $\rho \rightarrow \rho \exp(i\theta)$ [20]. Since all other coordinates are angles, i.e. ratios of lengths, only ρ becomes complex. If θ is sufficiently large both bound states and resonances are obtained with the bound state boundary condition of exponential fall-off of the radial wave function for large hyperradius. The resulting resonance energies are again complex numbers corresponding to positions and widths. For bound states any rotation θ can be used. One adiabatic potential is sometimes sufficient to describe the resonance without any complex rotation.

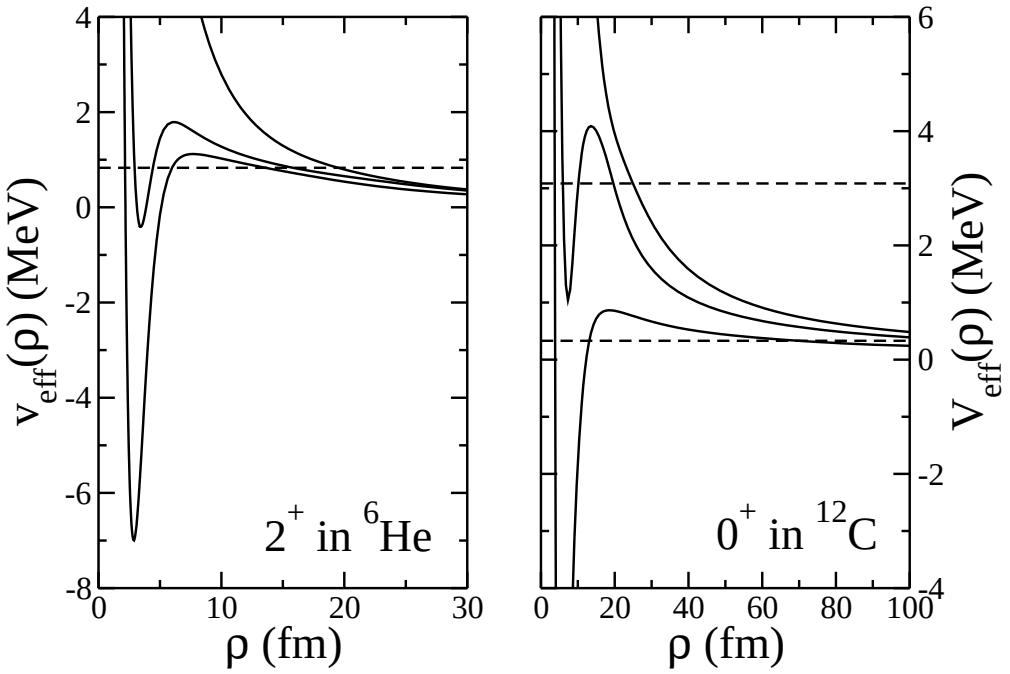

Fig. 1. The lowest adiabatic potentials as functions of ρ. Left side shows the 2^+ states in ^{6}He (^{4}He + n + n). The resonance energy (horizontal line) and the width are 0.824(25) MeV and 0.113(20) keV [23]. Right shows the 0^+ states in ^{12}C ($\alpha+\alpha+\alpha$). For the lowest two unbound states the energies (horizontal lines) and widths are, 0.369(10) MeV and 8.5(1.0) eV, 3.0(3) MeV and 3.0(7) MeV, see [24].

2.2 Resonance decay mechanisms

The full computation of S-matrix poles provides widths of the resonances. However, this quantum mechanical partial three-body decay width only gives the weighted sum of all amplitudes leading from the initial to the final state. The dominating path(s) defining the decay mechanism(s) are not revealed in the value of the width. Fortunately the model does contain such information [3] and we shall try to extract it.

The picture of sequential decay is very often used in data analyses [4–6,10]. The measurements provide the relative energy between pairs of fragments, i.e. the excitation energy of the corresponding two-body subsystem. The experimental definition of sequential decay is that this energy, properly extrapolated to small distances, matches a known resonance energy. The outcome is frequently that sequential decay is overwhelmingly dominating. This is perhaps not surprising since no other mechanism is included. However, careful comparison between experiment and R-matrix theory suggest that contributions of a different origin sometimes seem to be necessary [25].

At this point it may be appropriate to emphasize that any complete basis can be used to describe these decay processes occurring for positive energies in the continuum. A complete basis could be product functions of two complete two-body basis sets of the relative motion of (i) two particles and (ii) their center of mass and the third particle. This choice matches perfectly with the sequential decay process. However, other complete basis sets are possible for example the set of continuum three-body wave functions which includes the three-body resonances, or the rotated wave functions where the resonances explicitly are separated out [18]. The latter basis sets are more appropriate when the decay directly populates states which are complicated superpositions of the simple sequential decay basis. The best choice is not a matter of principles or decay mechanism, but a practical question of faster or slower convergence.

The adiabatic expansion method provides a complete basis consisting of the angular eigenfunctions. Each of these adiabatic eigenfunctions is a function of the hyperradius varying from small to large values, i.e. leading from initial to final state by a fully specified amplitude provided by the self-consistent adiabatic adjustment of the particles as the average size (hyperradius ρ) increases. This path could for example describe the two steps of a sequential decay process. However, it could also be a specific coherent superposition of more than one sequential process. It could also be something else like all particles proportionally increasing their mutual distances, or any other coherent or incoherent combination of relative motion. Clearly more combinations become possible when more than one adiabatic component contribute, but the principle is still the same, i.e. a specific weighted combination of paths from initial to final state. The great advantage is that the adiabatic eigenfunctions by definition are optimum choices for each distance.

Sequential decay seems intuitively most likely when a narrow two-body resonance offers an intermediate stepping stone. In turn this is most appropriate when the initial three-body resonance wave function has a very large overlap with the two-body resonance wave function multiplied by some function depending on the relative coordinate of the last particle. Then the decay towards larger distances would proceed in this configuration until other channels are populated. This typically occurs when other adiabatic potentials corresponding to different configurations cross. The crucial sizes of the related couplings are closely connected to the imaginary part of the two-body S-matrix pole which is half the width. The qualitative relation is that a small width means small coupling and therefore pronounced sequential decay through the initial two-body resonance.

In contrast direct decay is expected to dominate both for a large two-body resonance width implying strong couplings to other channels and when the initial three-body resonance wave function has no configuration similar to a two-body subsystem in a resonance. In the first case the decay path would

quickly change away from the sequential behavior and not come back. In the latter case the decay path can only change character and look like sequential decay if the adiabatic potentials couple strongly to precisely such a configuration. This is much more unlikely since many other channels also are open directly to the continuum.

The hyperspherical adiabatic expansion method includes simultaneously all decay channels, i.e. provides automatically the partial three-body decay width when the decay is either direct or sequential or any combination. Unlike other approaches no assumption is a priori made about the decay mechanism. All channels can be obtained in one computation. Thus we have the prerequisites for discussing the mechanism of three-body decay of a given resonance. The task could be to characterize different decay mechanisms and investigate under which conditions the corresponding paths are dominating. In particular, we would like to know if sequential decay dominates over direct decay or vice versa.

3 Realistic calculations

The schematic model with only Coulomb potential and centrifugal barrier provides indication of the dominating decay mode [17]. However, the short-range interaction is often decisive, i.e. when correlated intermediate configurations along the decay path minimize the dominating action integral. The adiabatic potentials are precisely constructed to carry such signature of the three-body structure as the system expands. Each potential could correspond to one dominating configuration, e.g. sequential decay where one two-body subsystem is in a favored resonance state while the third particle moves away. Different types of sequential decay can exist, i.e. via different two-body resonances in the same subsystem (coherent) or via different subsystems (incoherent). With one dominating potential the width can be reliably estimated by the (WKB) tunneling width. We shall illustrate by realistic examples.

3.1 Short-range potentials: $^6He(2^+)$

The first example is the well studied two-neutron Borromean halo nucleus, ^{6}He (^{4}He+n+n), where details of interactions and computational accuracy are available. Furthermore the analytically established asymptotic behavior of the adiabatic potentials is reached at relatively small distances since only the short-range interaction is present. Both the 0^+ ground state and the 2^+ excited state are rather well described as three-body states, see Fig. 2. The two-body subsystem of n+^{4}He has no bound states but a $p_{3/2}$-resonance, and

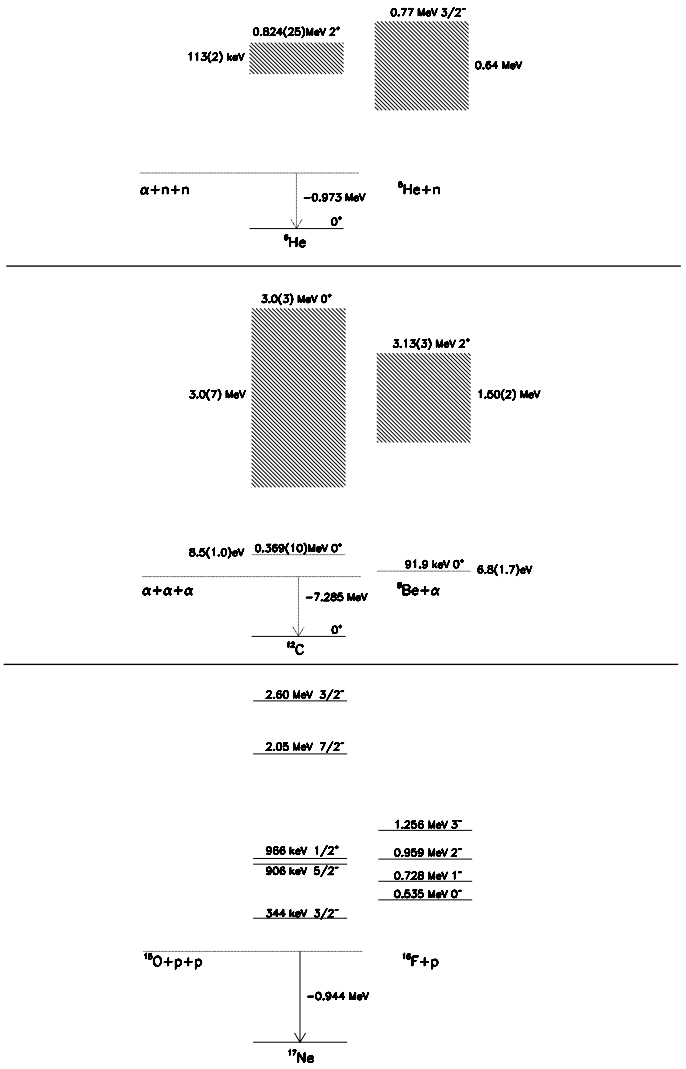

Fig. 2. The experimental low-energy spectra for ^{5}He, ^{6}He, ^{12}C, ^{8}Be, ^{17}Ne and ^{16}F. The data are from [23], [26], [27].

the two-neutron system has a virtual state at -0.14 MeV [19].

Then (parts of) the decay of the 2^+-state could be sequential via the broad ^{5}He-resonance or via α-emission leaving a two-neutron configuration behind. The lowest adiabatic potentials are shown in Fig. 1. The different numerical results are summarized in the second row of table 1. The full computation from the complex rotation method with (without) the weak three-body potential gives a resonance energy of 0.82 MeV (1.1 MeV) and a width of 0.12 MeV, which is remarkably close to the measured values [26]. These values are quoted as realistic in the third and fourth columns of table 1. Using only the lowest non-rotated adiabatic potential with the energy equal to 0.82 MeV the WKB estimate for the width [15] is 0.19 MeV (fifth column), where the uncertainty in the knocking rate alone can explain the deviation from 0.12 MeV. Therefore the wave function along the path defined by this potential reveals the decay mechanism by showing the structure continuously changing from small to large distances. In table 1 we also show the results corresponding to the schematic

Table 1
For the 2^+ resonance in ^{6}He, the two lowest 0^+ resonances in ^{12}C, and the $3/2^-$ and $5/2^-$ resonances in ^{17}Ne we give the corresponding energies and widths computed with the realistic calculations described in [15,20] (third and fourth columns), the width in the WKB approximation as described in [15] (fifth column), and using the schematic approaches assuming direct and sequential decay given in [17] (sixth and seventh columns). In the fourth row, the number in brackets corresponds to sequential decay through the 2^+ state in ^{8}Be. The last two columns are the experimental values. All the energies and widths are given in MeV.

	J^π	$E_{real.}$	$\Gamma_{real.}$	Γ_{WKB}	$\Gamma_{sch.}^{(Dir.)}$	$\Gamma_{sch.}^{(Seq.)}$	$E_{exp.}$	$\Gamma_{exp.}$
^{6}He	2^+	0.82	0.12	0.19	0.01	0.25	0.84	0.09
^{12}C	0_1^+	0.33	$2 \cdot 10^{-5}$	$6 \cdot 10^{-5}$	$\sim 10^{-6}$	$\sim 10^{-4}$	0.37	$8 \cdot 10^{-5}$
	0_2^+	4.3	0.64	0.4	0.2	0.7 (0.3)	3.0 ± 0.3	3 ± 0.7
^{17}Ne	$\frac{3}{2}^-$	0.34	—	$3.6 \cdot 10^{-12}$	$\sim 10^{-9}$	—	0.34	$< 2.5 \cdot 10^{-11}$
	$\frac{5}{2}^-$	0.82	—	$1.3 \cdot 10^{-10}$	$\sim 10^{-5}$	$\sim 10^{-5}$	0.82	$> 3 \cdot 10^{-10}$

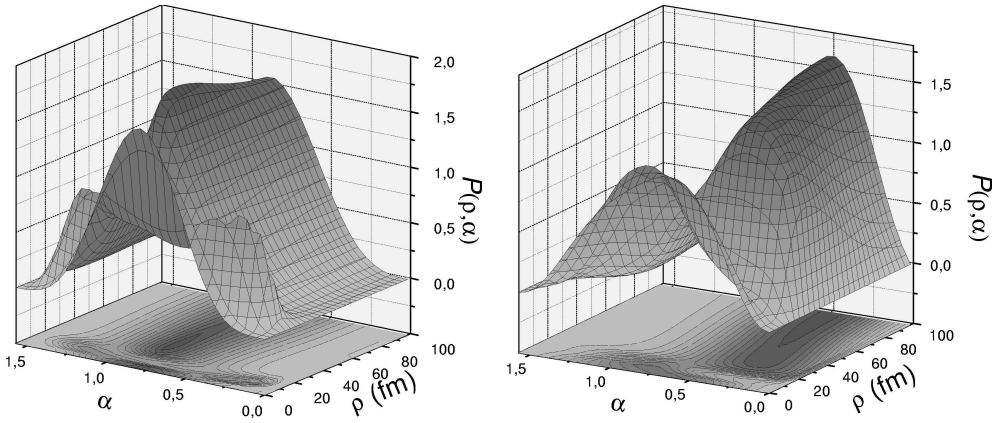

Fig. 3. The probability distribution for ^{6}He(2^+) for the lowest adiabatic potential as function of hyperradius ρ and α related to the distance by $r_{ik} \propto \rho \sin \alpha$, i.e. the distance between either the one neutron and core r_{nc} (left) or the two neutrons r_{nn} (right).

approaches for a centrifugal barrier potential as given in [17] (sixth and seventh columns). They refer to the direct decay and the sequential decay through the $p_{3/2}$ resonance in ^{5}He. In these calculations we have used a ratio between the outer and inner turning points of around 3, as suggested by the lowest adiabatic potential for this resonance shown in Fig. 1. The knocking rate multiplying the transmission coefficient is put equal to a typical value of 3 MeV/$\hbar$. These estimates suggest that the decay of the 2^+ resonance in ^{6}He could be sequential. However, this result is highly sensitive to the value of the ratio between the turning points, that for sequential decay could be very different from direct decay. A ratio equal to 5 gives an estimated width for the sequential decay similar to the one quoted for the direct decay.

The probability distributions shown in Fig. 3 are obtained by integration over all coordinates except the hyperradius and the distance between two of the

particles. When the distance refers to one neutron and the α-particle we see three peaks for small ρ, i.e. at small and large α corresponding to an α-particle spatially close to one of the neutrons and an intermediate $\alpha \approx \pi/4$ corresponding to a triangular configuration with equal distances between all three particles.

As ρ increases through and far beyond the barrier the probability appears to peak for the triangular configuration. Sequential decay through the two-body resonance can not be seen. This is consistent with the rather low barrier height observed in Fig. 1, which does not leave any room for a flat region above the two-body resonance at 0.77 MeV. The generalized centrifugal barrier is already lower when ρ is around 15 fm. Thus the short-range interaction and the broad two-body resonance seems to make it advantageous to take the direct decay road to the continuum. The two-body energy is also rather close to the three-body resonance energy, but the main reason is that the third particle can feel the short-range interaction until distances outside the low and thin barrier.

To illustrate the other possible sequential decay mode of α-emission we also show in Fig. 3 the probability as function of ρ and the distance between the two neutrons. At small ρ the dominating feature is a peak corresponding to roughly equal distance between the two neutrons and their center of mass and the α-particle. This distribution reflects the same initial triangular resonance structure as seen in the other coordinate system in Fig. 3. As ρ increases the probability peaks at relatively small values of the α-coordinate. However, applying the proper mass scaling we find that the distance between the two neutrons is comparable to the neutron-α distances. Thus from both plots we find that all three particles on average move apart with roughly equal distance between all pairs. This is compatible with direct decay into the three-body continuum. Neither the s-wave attraction (virtual state) between the neutrons nor the p-wave resonance in the $n-\alpha$ system is capable of producing a substantial sequential component.

The structure of the wave function is characterized by the quantum numbers of its different components. We show in Fig. 4 how they change as ρ increases. By far the largest component at small distances is a $p_{3/2}$ neutron-α structure coupled to the other neutron in precisely the same relative state around the common center of mass. This structure is maintained in the non-classical region, but changes quickly outside the barrier where all three possible different p-wave combinations become equally probable. This again confirms the previous observation that no two-body subsystem is used as a stepping stone on the path to full separation of all particles. If for example the $p_{3/2}$ resonance first would be populated the $p_{1/2}$ neutron-α component should have been smaller at the large distances. Now instead all particles simultaneously move outside the range of the short-range interaction and preference for such fine-structure is lost.

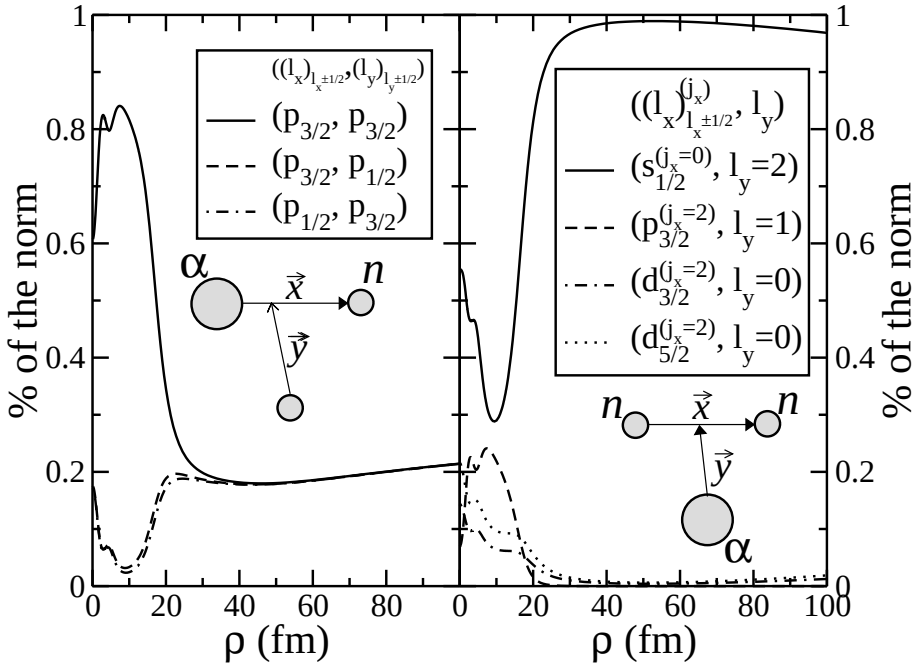

Fig. 4. The fraction of different components in the lowest adiabatic potential as function of ρ for ^{6}He(2^+). The angular momenta are specified by ℓ_x, j_x, ℓ_y, j_y and $J = 2$. Left x refers to the neutron-α system and y to its center of mass motion relative to the other neutron. We give the (x, y) components on the figure as ℓ_j. Right x refers to the two-neutron system and y to its center of mass motion relative to the α-particle. We give the (x, y) components on the figure as $\ell_j^{(j_1)}$, where j_1 is the angular momentum quantum number obtained by coupling of ℓ_x and the neutron spin of 1/2.

It may be informative to express the components in terms of a different coupling scheme where the relative motion of the two-neutron system first is established and then coupled to the motion of the α-particle. As seen in Fig. 4 at small distances a number of components of comparable magnitudes are present, but immediately outside the barrier and at larger distances only one component remains, i.e. the two neutrons in relative s-states coupled to angular momentum zero moving around the α-particle in a d-state. This structure could of course be called a dineutron-α d-state, and the decay could correspondingly be mistaken for a sequential decay via emission of an α-particle. However, no intermediate two-body structure is populated. Instead all distances increase proportionally until the decay is completed and all particles are free. This is because the short-range interaction already lowered the barrier for direct emission to a lower energy than for the intermediate configuration.

3.2 Symmetric cases with Coulomb potential: $^{12}C(0^+)$

A relatively simple Coulomb dominated structure is found in the celebrated second 0^+-state in ^{12}C which approximately can be described as a three-body resonance [3]. The two-body subsystem can then only be ^{8}Be with the 0^+ ground state, see Fig. 2. These narrow two and three-body widths are both due to prominent Coulomb barriers. The higher-lying 0^+-state is computed to be at the energy 4.3 MeV with a width of 0.6 MeV [20]. It could then decay sequentially via the 2^+ rotational-like state in ^{8}Be at about 3 MeV.

To study the decay mechanism we again use the lowest adiabatic potentials shown in Fig. 1. The fine-tuning with the three-body potential reproduces the measured resonance energy and the width approximately in full computations with several adiabatic potentials and complex rotation. Using only the lowest non-rotated adiabatic potential with the correct energy of 0.37 MeV for the lowest 0^+-state we find the WKB width of about 0.060 keV, i.e. three times larger than the full computation [3] and about eight times larger than the measured value. For the next 0^+ resonance the experimental energy of 3.0 MeV leads to a WKB width around 8 keV which is much smaller than the experimental value of 3.0 MeV. The computed energy of 4.3 MeV leads instead to the much larger WKB width of 0.4 MeV, because now the two turning points are very close to each other and the barrier penetration is much more probable. This width is comparable to 1.1 MeV found in [14] where the inconsistency between position and width also was noticed. It is encouraging that this larger computed energy of about 4 MeV is in better agreement with recent experimental values [28]. These results are collected in the third and fourth rows of table 1.

The results corresponding to the schematic calculations described in [17] are also given. These estimates depend only on the ratio between the outer and inner turning points. This ratio is taken equal to 4 and 2 for the first and second 0^+ resonances, respectively. These values are suggested from the effective potential for each of the two resonances shown in the right part of Fig. 1. The knocking rate is again taken equal to 3 MeV/$\hbar$. For the second 0^+ resonance two estimates for the case of sequential decay are given, one for decay through the lowest 0^+ state in ^{8}Be, and also, in parenthesis, the one assuming sequential decay through de 2^+ resonance in ^{8}Be. The absolute values from the schematic model deviate by less than about one order of magnitude from the experimental values.

The lowest 0^+ resonance wave function has a probability of more than 95 % arising from the first adiabatic potential. We show in Fig. 5 its structure revealed by the probability distribution as function of hyperradius and distance between two α-particles. At small ρ the dominating peak is at $\alpha \approx \pi/4$ con-

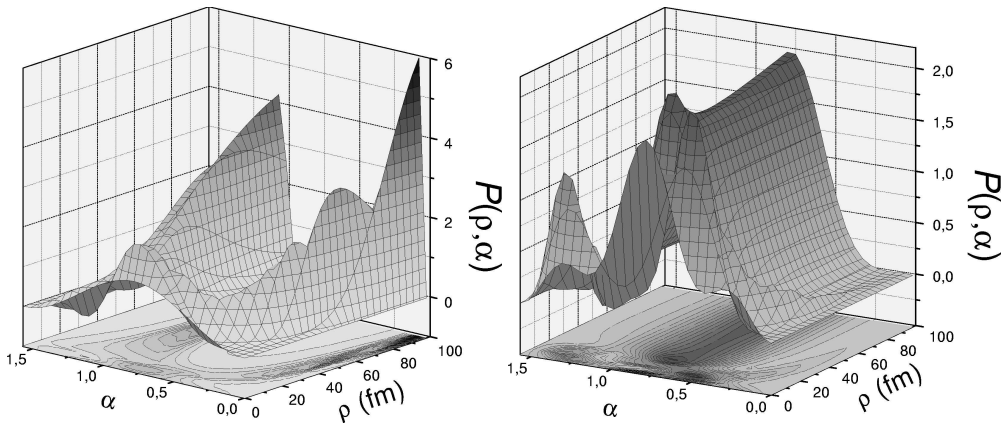

Fig. 5. The probability distribution for ^{12}C(0^+) for the first (left) and second (right) adiabatic potential as function of hyperradius ρ and α related to the distance between two α-particles.

sistent with a diffuse elongated structure. As ρ increases this peak is divided into two separated ridges, i.e. one at very small α corresponding to two close-lying particles and one at $\alpha \approx 1$ consistent with the configuration arising from symmetrization of this classical structure.

The probability distribution reflects sequential decay as expected from a decay where the short-range attraction can be exploited until one Coulomb interaction is strongly reduced by removal of one of the charged particles. This sequential decay mechanism is only favored due to the short-range interaction which is responsible for the ground state structure of ^{8}Be. Otherwise direct decay would have been as probable as discussed for schematic models [17]. This conclusion is strongly depending on the total energy of the decay and its possible division into the two sequential steps.

The second excited 0^+-resonance has a probability of more than 98 % arising from the second non-rotated adiabatic potential. The corresponding probability distribution is also shown in Fig. 5. At small ρ we now see three peaks revealing a different structure. Nevertheless, as ρ increases only one prominent ridge remains at $\alpha \approx \pi/4$ corresponding to equal scaling of all distances between pairs of particles. This direct decay mechanism is not overshadowed by sequential decay via the excited 2^+ rotational-like state in ^{8}Be at about 3 MeV. Apparently the short-range interaction cannot compete when the penalty for angular momentum first must be payed.

The structure of the resonance wave functions can be seen in Fig. 6 where the quantum numbers of the components are given as function of ρ. The quickly changing contribution at small ρ is due to coupling and subsequent admixtures of the two close-lying adiabatic potentials in this region. For the first 0^+-resonance the partial s-waves dominate for ground state distances as also found in [14]. As ρ increases beyond about 25 fm the s-wave contribution decreases substantially while correspondingly the higher partial waves contribute more as the sequential decay structure is changing into the structure of three free α-particles. This is apparently achieved most efficiently by exchanging angular

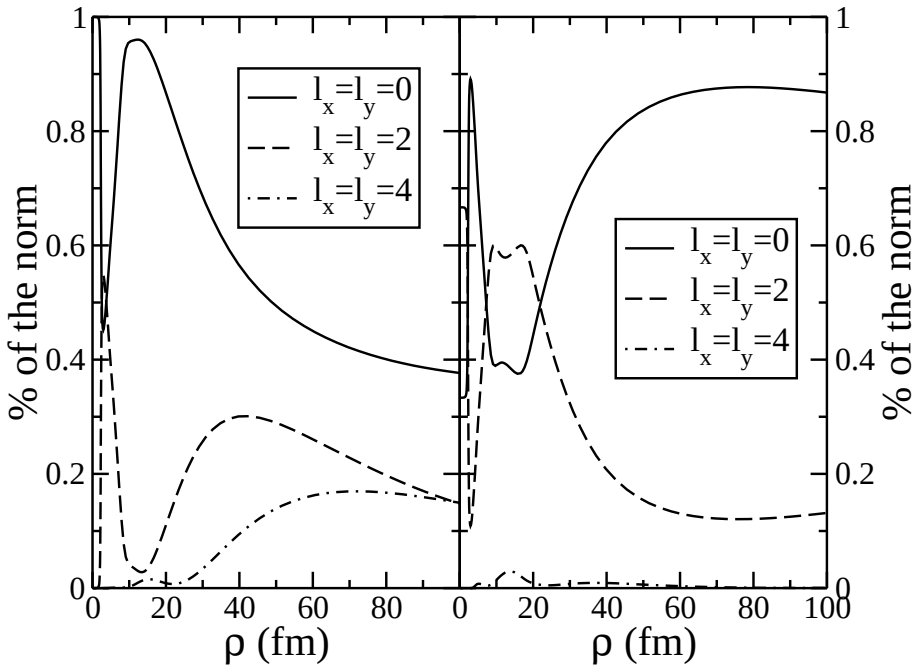

Fig. 6. The fraction of different components in the first (left) and second (right) adiabatic potential as function of ρ for ^{12}C(0^+). The partial orbital angular momenta are equal since they couple to a total of 0 and all intrinsic spins are zero.

momenta between the subsystems.

In comparison the second 0^+-resonance has a very different behavior as function of ρ. The small ρ-admixture has the same fast variation, but in the intermediate region s and d-waves are about equally probable. The d-waves of about 50% in the ground state are apparently smaller than in [14] where they dominate. For the decay process this variation may be interpreted as two simultaneously contributing sequential decays via 0^+ and 2^+-states in ^{8}Be. However, this interpretation is not comparable with the probability distribution in Fig. 5. At larger distances the exchange of angular momenta is no longer needed in this direct decay and the s-wave probability quickly increases towards unity. All distances scale proportionally and all partial waves can as well assume their lowest possible values reflected in the decrease of d-waves while all higher partial waves remain small.

Even if angular momentum 2 is populated at intermediate distances sequential decay through the 2^+ state in ^{8}Be is not automatically preferred. The large two-body width indicates direct decay since an α-emission quickly would be followed by a two-body decay occurring already at distances comparable to the ^{12}C radius [17]. The dominating s-wave component at larger distances also contradicts 2^+ sequential decay, but allows the conclusion from experiments of

dominating 0^+ sequential decay [29]. The measured energy spectra still seems to contradict the direct decay as exhibited by the probability distribution in Fig. 5. One complication is that the coherent population of the two 0^+ resonances in experiments produce inseparable contributions. However, the fast increase of the $l = 0$ component probably must be interpreted as sequential decay if the wave function is expanded on a basis of ^{8}Be-states multiplied by distorted waves. This is implicit in the usual analysis using R-matrix theory.

3.3 Asymmetric cases with Coulomb potential: ^{17}Ne(^{15}O+p+p) resonances

Beyond or at the proton dripline peculiar structures are possible, because the Coulomb repulsion can create a barrier which confines otherwise unbound charged particles to remain at short distances in states of long lifetimes. The lightest Borromean two-proton nucleus ^{17}Ne has several such resonance states, see Fig. 2. The ground state and the two first excited states are all essentially of three-body structure [15]. The Borromean nature prohibits proton decay from the ground state but also the $3/2^-$ state has too low an energy to allow proton emission. In contrast the $5/2^-$ state has sufficient energy to emit a proton and a two-step sequential decay in its pure form is in principle allowed, see Fig. 2.

The lowest adiabatic potentials are shown in Fig. 7 as functions of ρ for $3/2^-$ and $5/2^-$. The $3/2^-$ resonance is dominated by the lowest-lying potential at small distances. This potential has the remarkable behavior of being very flat in a relatively large region, reaching at least to $\rho = 25$ fm after crossing other potentials. A two-body substructure with the third particle far away would produce this behavior. The slow decrease for ρ larger than about 8 fm has to be present due to the long-range Coulomb repulsion between the third particle and the subsystem. Also the decreasing centrifugal barrier potential should be visible in this potential. The other adiabatic potentials decrease more regularly as expected when the short-range interaction has vanished. These structures then correspond to configurations where all three particles are spatially separated.

The two-proton decay of the $3/2^-$ state cannot be strictly sequential, since the energy is below the energy of the unstable ground state of ^{16}F. This does not prevent the decay from proceeding via the energetically favorable path described by the lowest adiabatic potential until at some point energy conservation eventually dictates that also this two-body structure must be broken. The decay mechanism is then best described as virtual sequential decay through one of the ^{16}F states. This mechanism is equivalent to the decay through the tail of an energetically unaccessible state (a ghost) described by other authors to contribute significantly [12]. The corresponding probability distribution is shown in Fig. 8. At small distance only one prominent peak is present but

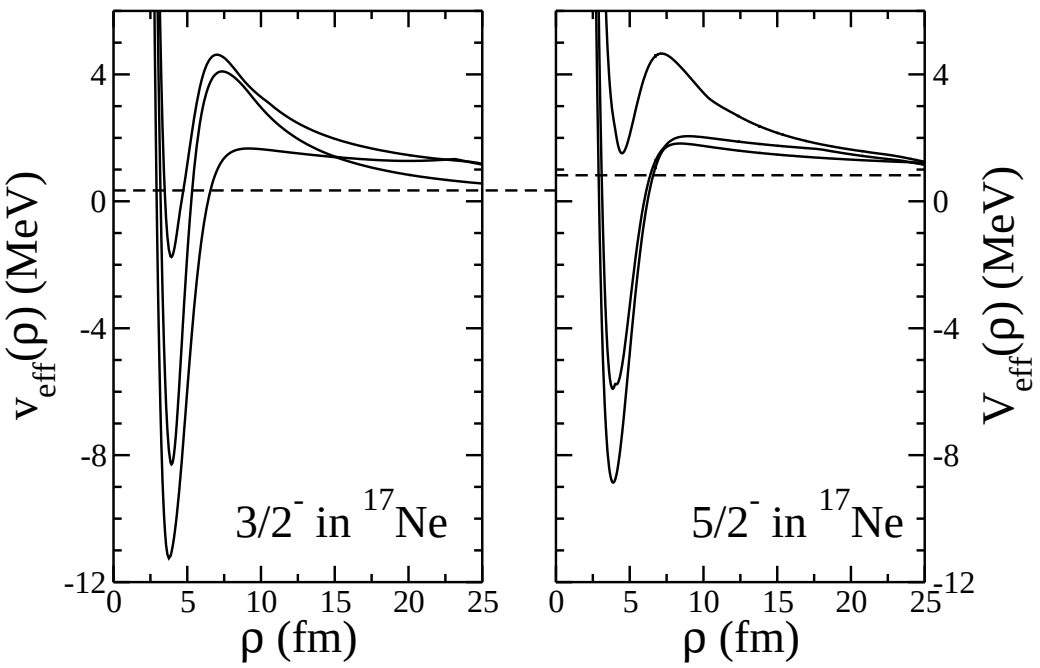

Fig. 7. The lowest adiabatic potentials as function of ρ for the states of $\frac{3}{2}^-$ (left) and $\frac{5}{2}^-$ (right) in ^{17}Ne(^{15}O+p+p). The resonance energies at 0.34 MeV and 0.82 MeV are indicated by the horizontal lines.

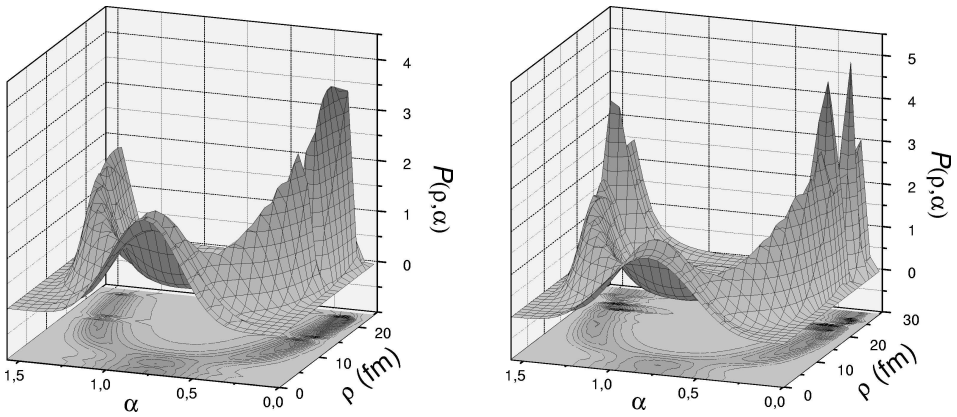

Fig. 8. The probability distribution for the dominating adiabatic potentials of ^{17}Ne($\frac{3}{2}^-$) (left) and ^{17}Ne($\frac{5}{2}^-$) (right) as function of hyperradius ρ and α related to the distance between the proton and the ^{15}O-core.

quickly this develops into two ridges at small and large distances between one proton and the core. The ridge at large α corresponds to the large distance between core and emitted proton.

We know that the resonance at small distance is dominated by components where the proton-core two-body configurations are of *sd*-structure [15]. Two

s-waves cannot couple to 3/2 due to antisymmetry of the two protons. The angular momentum of 3/2 is reached when both s and d-resonances in ^{16}F are maximally exploited. Two decay paths seem to be advantageous, i.e. sequential decay via either the s-state at 0.53 MeV or the d-state at 0.95 MeV in ^{16}F. In both cases the first step would only amount to removal of one proton while the other is left in the same state. The energies of these intermediate configurations differ by 0.42 MeV, but also by the centrifugal potential for the relative motion between the emitted proton and the ^{16}F s or d two-body state. Since the s-state is lowest the centrifugal barrier from the additional two units of $\hbar$ compensates at intermediate distances almost precisely for the energy difference of 0.42 MeV.

The potential energy of the flat region is about 0.25 MeV larger than obtained by adding Coulomb and centrifugal contributions to the two-body states of the corresponding ^{16}F configurations. Thus the intermediate state cannot be precisely the structures of the ^{16}F-resonances. The most crucial decay path is via the dominating potential followed through the crossing at 15 fm up to $\rho = 25$ fm and then taking the lowest potential to the classical turning point. The corresponding WKB estimate (see table 1) for the width obtained is found to be $\simeq 3.6\times10^{-12}$ MeV consistent with the experimental constraints from the γ-decay [5,15]. In contrast this is far from the estimate of $\simeq 1.2 \times 10^{-19}$ MeV obtained in [13] where the method essentially excludes contributions from the virtual sequential decays, which is overwhelmingly dominating in our width computation. Furthermore, the chosen structure of the spin-dependent two-body interaction in [13] produces inseparable admixtures of proton-core $d_{3/2}$ and $d_{5/2}$-states within the three-body wave function [30]. The energy order of the $3/2^-$ and $5/2^-$ states is reversed and the results are therefore questionable. The schematic model gives a larger value for the direct decay, while sequential is forbidden by energy conservation. The ratio between the outer and inner turning points is taken equal to 7 (taken from the effective potential in Fig. 7), and the knocking rate again equal to 3 MeV/$\hbar$. The value obtained is larger than in the WKB calculation and the experiment because the strong interaction substantially increases the barrier width due to the virtual decay mechanism, where the two-body state in the decay is populated up to very large distances.

Our estimates indicate that the decay paths via the s or d-states of ^{16}F are of comparable importance. The lowest adiabatic potential shown in Fig. 8 contains the most favorable combination obtained by the condition of adiabatic energy minimization. The contributions from the different components are revealed by the probabilities shown in Fig. 9. Below the barrier the ^{16}F d-state remains steady on about 50% while the s-state population in the dominating adiabatic potential decreases from 50% down to about 20% as ρ increases up to 25 fm. These results demonstrate first the virtual sequential decay mechanism and second that one adiabatic potential by clever coherent superposition

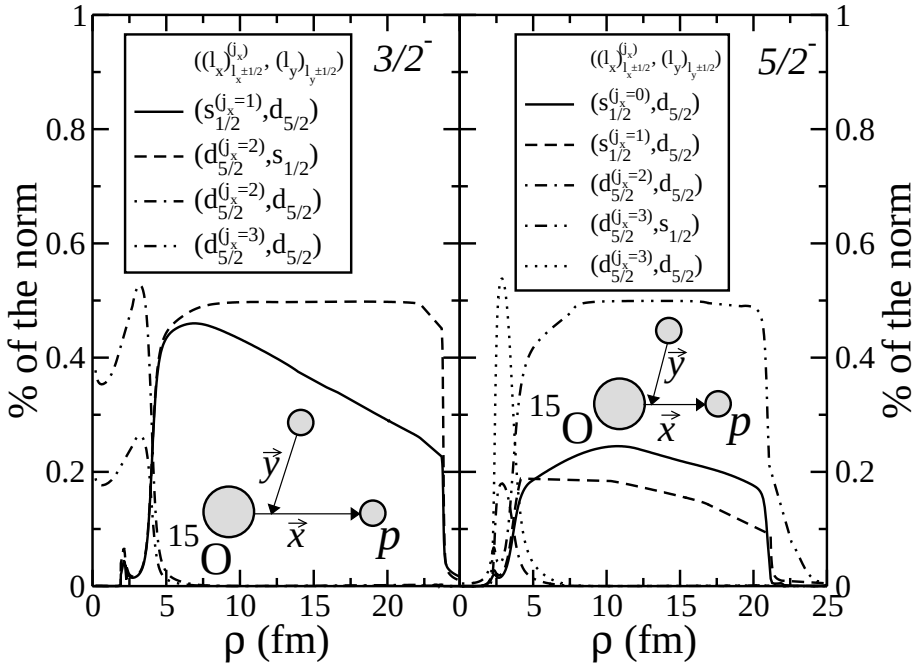

Fig. 9. The fraction of different components for the dominating adiabatic potentials as function of ρ for ^{17}Ne($\frac{3}{2}^-$) (left) and ^{17}Ne($\frac{5}{2}^-$) (right). The notation is as in Fig. 4.

in itself simultaneously is able to describe two different sequential decays via two different ^{16}F states. The important channels are already included in one adiabatic potential.

The $5/2^-$ resonance in ^{17}Ne is energetically able to decay sequentially via the two lowest states of ^{16}F, see Fig. 2, but in both cases the centrifugal barrier must then correspond to angular momentum 2. We show the adiabatic potentials in Fig. 7 where we find two low-lying potentials with long relatively flat regions at intermediate distances. The energies correspond almost to a constant two-body energy combined with the decreasing Coulomb and centrifugal potentials arising from the emitted proton. The resonance wave function has probabilities of 77% and 17% on the first and second of these potentials, respectively. The probability distribution for the dominating component is shown in Fig. 8. The one-peak distribution at small ρ develops into two ridges at small and large proton-core distances. This is again the signature of a sequential decay. The corresponding WKB width is found to be $\simeq 1.3\times10^{-10}$ MeV (table 1) again competing with γ-decay. In comparison [13] obtained $\simeq 1.2\times10^{-11}$ MeV and $\simeq 5\times10^{-9}$ MeV for direct and sequential decay, respectively. These results are comparable to our estimate of the width, i.e. 10 (2) times smaller (larger) for direct (sequential) decay.

The effective potentials in Fig. 7 suggest a ratio between the outer and inner turning points of around 5 for the $\frac{5}{2}^-$ resonance. The values of the widths given in table 1 corresponding to the schematic calculations have been obtained using this value for the ratio of turning points. The sequential width by proton emission has been computed assuming decay through the lowest resonance in ^{16}F. The widths obtained in this way for the direct and sequential decay are very similar, and a not very significant change in the parameters (for instance the knocking rate that is taken equal in both cases) could make one width or the other to be the largest. So, this estimate does not permit to determine clearly in this case which of the decays is preferred. Again the schematic model gives relatively large widths because the strong interaction in the realistic calculations maintain the two-body resonance populated in the intermediate step up to very large distances. This mechanism is the same for allowed and virtual sequential decay and in both cases the barrier width is significantly increased.

The intermediate ^{16}F two-body state could be either 0^- and 1^- as allowed by energy conservation, or it could be 2^- and 3^- if virtual sequential decay is favored as for the $3/2^-$ state, see Fig. 2. Neither 0^- nor 1^- can be combined with an s-wave of the emitted proton to produce the initial $5/2^-$ state. Then there seems to be no reason to choose the more expensive path via the 1^- state. On the other hand both the 2^- and 3^- states can combine with an s-wave and produce $5/2^-$. For these the least expensive combination is then the 2^- state. Thus we can expect coherent contributions from sequential decay through the 0^- state and virtual sequential decay through the 2^- state.

The optimum combination is found by the dominating adiabatic potential and the corresponding components are shown in Fig. 9 as functions of ρ. As for the $3/2^-$ state below the barrier the d-state of ^{16}F remains steady on about 50% while the two s-state populations each of about 20% have a tendency to decrease with ρ. The sudden decrease to zero at about 22 fm is due to the crossing of the two adiabatic potentials. The probabilities would otherwise smoothly continue on the other potential.

The two $7/2^-$ and $9/2^-$ resonances in Fig. 2 are probably not as clean three-body states since one core excitation with an appropriate angular momentum and parity also is energetically favorable. Ignoring such a core-contribution three-body computations show smaller and thinner barriers due to the higher energies. The flat regions under the barriers are no longer present. On the other hand the probability distributions behave qualitatively as for the two lower-lying resonances. This again then strongly indicates sequential decays. The larger angular momenta now require two d-states and the intermediate ^{16}F states must then be either 2^- or 3^-. The Coulomb and centrifugal barrier potentials are the same for both these cases and therefore expected to provide roughly equal contributions. Also for these resonances the short-range

interaction is crucial for the behavior of the dominating adiabatic potentials. The reason is again that one proton can be emitted while the attraction is exploited in the remaining ^{16}F state. In this way the short-range interaction is decisive for the decay mechanism

4 Summary and conclusions

As in the companion paper [17] we investigate the decay of low-lying continuum states into three-particle final states. We focus on the illuminating relation between the partial three-body decay widths and the decay mechanisms. We assume that the three fragments are formed before entering the barrier at sufficiently small distances to allow the three-body treatment. This is analogous to the two-body α-decay and seems to be a reasonable working hypothesis which however for some structures may turn out to be inaccurate. We are then left with a three-body problem consisting of the three interacting particles eventually appearing in the final state. By definition the energy is positive measured relative to the break-up threshold. The necessary technique must therefore be able to describe three-body continuum structure and in particular three-body resonances. It is worth emphasizing that the initial state can be a complicated many-body state with three-body decay as one, more or less, probable decay channel.

The hyperspherical adiabatic expansion method is an efficient tool to compute bound states and resonances when combined with the complex rotation method. This means that rather accurate calculations of three-body resonance widths are available. Furthermore, one adiabatic potential is often dominating a given resonance and therefore in itself providing a reasonable estimate of the width. The wave function along this adiabatic potential then presents a continuous connection between initial and final states. It can be viewed as a classical path providing the largest contribution to the width. In principle other potentials should also be included to go beyond the classical treatment of this coordinate. This is achieved by the complex rotation method. Even with one adiabatic potential all other coordinates are treated quantum mechanically correct by including a distribution of amplitudes coherently adding up to produce this individual adiabatic potential.

We introduce the short-range interaction in realistic calculations. Direct decay is demonstrated for ^{6}He. The intermediate configurations turn out to be at higher energies than along the direct path. The Coulomb dominated decays, exemplified by two 0^+ states at different energies in ^{12}C, are predicted to be either sequential (low energy) or direct (high energy). Two-proton decays of the proton dripline nucleus ^{17}Ne is strongly sequential for the two lowest excited $3/2^-$ and $5/2^-$ resonances. However, the intermediate two-body state

in ^{16}F has too high an energy to be populated from decay of the 3/2-state. Still the mechanism is clearly sequential by keeping proton and core spatially close up to very large average distances. This can only be achieved by exploiting the attractive two-body short-range interaction. The process is called virtual sequential decay. It is then not surprising that also the 5/2-state favors sequential decay.

In conclusion we have demonstrated how to classify and characterize various decay mechanisms, i.e. sequential, direct and virtual sequential. We illustrated by elaborate realistic computations. The intermediate configurations strongly indicate which basis is most efficient in analyses and interpretations of experimental data. The three-body structure can be fully explained in a complete basis chosen as the intermediate two-body sequential decay states multiplied by distorted waves for the third particle. This does not imply that all decays are sequential. Another complete three-body basis like the adiabatic states can also be used and in this paper demonstrated to include both aspects in a natural way.

References

[1] Proc. Conf. on Correlations of Particles Emitted in Nuclear Reactions, ed. C.D Goodman, Rev. Mod. Phys. **37** (1965) 327.

[2] A.S. Jensen, K. Riisager, D.V. Fedorov and E. Garrido, Rev. Mod. Phys. **76** (2004) 215.

[3] D. V. Fedorov and A. S. Jensen, Phys. Lett. **B 389** (1996) 631.

[4] R.A. Kryger et al., Phys. Rev. Lett. **74** (2002) 860.

[5] M.J. Chromik et al., Phys. Rev. **C 66** (2002) 024313.

[6] B. Blank, J. Giovanazzo and M. Pfützner, C.R. Physique **4** (2003) 521.

[7] C.R. Bain et al., Phys. Lett. **B 373** (1996) 35.

[8] H.O.U. Fynbo et al., Nucl. Phys. **A 628** (2000) 38.

[9] J. Gomes del Campo et al., Phys. Rev. Lett. **86** (2001) 43.

[10] H.O.U. Fynbo et al., Phys. Rev. Lett. **91** (2003) 082502.

[11] B.A. Brown and F.C. Barker, Phys. Rev. **C 67** (2003) 041304.

[12] B.A. Brown, F.C. Barker and D.J. Millener, Phys. Rev. **C 65** (2002) 051309.

[13] L.V. Grigorenko, I.G. Mukha, and M.V. Zhukov, Nucl. Phys. **A 713** (2003) 372.

[14] C. Kurokawa and K. Kato, Nucl. Phys. **A 738** (2004) 455.

[15] E. Garrido, D.V. Fedorov and A.S. Jensen, Nucl. Phys. **A 733** (2004) 85.

[16] D. V. Fedorov, A. S. Jensen and H.O.U. Fynbo, Nucl. Phys. **A 718** (2003) 685c.

[17] E. Garrido, D.V. Fedorov, A.S. Jensen and H.O.U. Fynbo, Nucl. Phys. **A**, in press.

[18] T. Myo, K. Kato, S. Aoyama and K. Ikeda,, Phys. Rev. **C 63** (2001) 054313.

[19] E. Garrido, D.V. Fedorov, and A.S. Jensen, Nucl. Phys. **A 708** (2002) 277.

[20] D.V. Fedorov, E. Garrido, and A.S. Jensen, Few-body Systems **33** (2003) 153.

[21] E. Nielsen, D.V. Fedorov, A.S. Jensen and E. Garrido, Phys. Rep. **347** (2001) 373.

[22] A. Cobis, D.V. Fedorov and A.S. Jensen, Phys. Rev. Lett. **79** (1997) 2411.

[23] D.R. Tilley et al., Nucl. Phys. **A 708** (2002) 3.

[24] F. Ajzenberg-Selove, Nucl. Phys. **A 506** (1990) 1.

[25] F.C. Barker, Phys. Rev. **C 68** (2003) 054602.

[26] F. Ajzenberg-Selove, Nucl. Phys. **A 490** (1988) 1.

[27] V.Guimarães et al., Phys. Rev. **C 58** (1998) 116.

[28] H.O.U. Fynbo et al., Nucl. Phys. **A 738** (2004) 59.

[29] D. Schwalm and B. Povh, Nucl. Phys. **89** (1966) 401.

[30] E. Garrido, D.V. Fedorov and A.S. Jensen, Phys. Rev. **C 68** (2003) 014002.